AE-393
UDC 620.179.1
539.1.074.55
621.039.516.22

AE-393

A Gamma Scanner Using a Ge(Li) Semi-Conductor Detector, with the Possibility of Operation in the Anti-Coincidence Mode

R.S. Forsyth and W.H. Blackadder

AKTIEBOLAGET ATOMENERGI
STUDSVIK, NYKÖPING, SWEDEN 1970

A GAMMA SCANNER USING A Ge(Li) SEMI-CONDUCTOR DETECTOR, WITH THE POSSIBILITY OF OPERATION IN THE ANTI-COINCIDENCE MODE

R S Forsyth and W H Blackadder

SUMMARY

A fuel element transport flask has been modified as a facility for gamma scanning irradiated fuel elements up to a length of 75 cm. By means of a Ge(Li) semi-conductor detector, satisfactory activity profiles along the specimens have been obtained, permitting the location of individual fuel pellets.

An annular plastic detector surrounding the Ge(Li) detector allows operation of the spectrometer in the anti-coincidence mode, and reduction of the Compton continuum by about 50 % has been obtained.

Printed and distributed in April 1970.

LIST OF CONTENTS

1. INTRODUCTION

In previous reports in this series, (1 - 3) the use of a Ge(Li) semiconductor detector for the determination of the activities of gamma-emitting fission products in both axial and diametral scanning experiments has been described. The main energy range of interest in these experiments has been that between about 400 - 850 keV, where photopeaks from Zr-95, Nb-95, Cs-137, Ce-144 and Ru-106 can be resolved and measured.

However, certain features of the spectrum at higher energies are also of interest when examining reactor fuel: there are difficulties in determining the activity in the 696 keV peak due to Ce-144 after normal cooling times, since the photopeak is usually small compared with the peaks due to Zr-95 and Nb-95, which lie at slightly higher energies, and with the background. The Ce-144 photopeak at 2190 keV, on the other hand, is usually clearly resolved and gives a good peak to background ratio, although the counting times required are rather longer.

The 2190 keV peak gives rise to a double-escape peak at 1168 keV, the ratio between the two counting rates being determined by the dimensions of the detector when viewing a narrow collimated beam. The proximity of this double-escape peak to the 1050 keV peak from Ru-106 suggests a further method for estimating the fraction of fissions in U-235 and in Pu-239, in fuels where both types of fission reactions have occurred. Since the fission yields (4) for Ru-106 are higher in Pu-239 than in U-235 (4.57:0.38) while the reverse is true for Ce-144 (3.79:6.0), the ratio of the counting rates at 1050 and 1168 keV could be a sensitive measure of the relative fission rates, if sufficient details are known of the irradiation history. For this purpose, however, a larger detector would be required than that previously available in order to attain higher photopeak counting efficiencies at higher energies.

It was also planned to examine photopeaks at energies lower than 400 keV in diametral scanning experiments on short-cooled, slightly-irradiated specimens, where many fission products of interest give peaks between 80 - 380 keV. Measurement of photopeaks within this energy range, and even higher, is often made uncertain by the presence of the substantial Compton continuum under the peaks.

Both these improvements, of course, could be effected by the use of a larger Ge(Li) detector in conjunction with a scintillation detector operated in anti-coincidence. For our purposes, however, which involved the ability to transfer the detector system readily from one location (for axial scanning experiments) to another (for diametral scanning experiments), some compromises would be necessary to obtain a system that was fairly robust, not too heavy or of too intricate construction, but capable of giving a useful improvement in spectrum quality.

At the same time as these possibilities were being considered, a large 14 tonne transport flask, which had been used previously for bentcrystal diffraction experiments, became available. This transport flask has been modified and now represents a gamma scanning facility capable of handling irradiated experimental fuel rods of lengths up to 75 cm. It is the purpose of this report to describe this facility and the anti-coincidence detector system, and to give examples of typical results obtained.

2. GAMMA SCANNER

Two views of the modified transport flask and the gamma spectrometer are shown in Figs. 1 and 2. In the first figure, one of the lifting lugs at the top of the flask, the supporting trolley which can be accurately positioned in front of the detector, and the driving mechanism can be seen. Fig. 2 shows how the semi-conductor assembly is inserted into the annular plastic shield detector.

A sketch of the flask itself (not to scale) is shown in Fig. 3 a. The outer walls of the flask are of 350 mm thick steel with an inner liner of 56 mm thick lead, and the centre of the base is of 250 mm thick lead. The central guide tube shown in the sketch, which had been specially selected to have minimum bowing and the best possible diameter tolerance limits along the length, was cemented into position at two points to give maximum rigidity. By these measures, it was hoped to maintain a constant geometry of the fuel rod with respect to the collimator.

The aluminium specimen holder shown in Fig. 3 b, is capable of taking fuel rods up to 750 mm in length: the outside diameter of the ends is such as to ensure a good fit inside the guide tube. The upper end secures tightly into the end of the guide tube by means of a spring-loaded push fitting.

Fig. 3 c shows a sketch of the collimator used, made of lead in a steel liner. The total length was 300 mm, with a slit 20 mm x 2 mm, oriented horizontally so as to view completely across the fuel rod diameter.

The driving mechanism shown in Fig. 1, gives a choice of two scanning speeds: 10 mm or 20 mm per minute. The position of the fuel rod with respect to the collimator slit can be read off a steel tape attached to the driving chain to an accuracy of 1 - 2 mm.

After removing the driving mechanism, the whole flask can be lifted by crane and swung into a horizontal position by means of a specially-constructed cradle arrangement. From this it can be taken by truck to the concrete high-active cells where replacement of the fuel rod can be effected rapidly and fairly easily.

3. DETECTOR SYSTEM

The Ge(Li) detector, manufactured by the Section for Instrumentation of AB Atomenergi, is a rectangular parallelepiped of dimensions 30 mm length, 14 mm width and 10 mm height. The naked detector is placed on a horizontal platform at the end of the supporting bar in the cryostat head, so that the p-n junction is horizontal and parallel to the supporting surface, with the n-side layer at the top. The depth of the n-type layer is 1.7 mm, of the compensated layer 6.5 mm, and of the p-type layer 1.8 mm. Thus the sensitive volume of the detector is 2.8 cm^3, but in this work, the whole volume of the detector was not exposed to the incident gamma beam. The collimated beam entered the front side of the detector horizontally and passed through the 30 mm thick detector. In order to give reasonable robustness, the aluminium hood around the detector is 2 mm thick except for the front window where it is only 0.5 mm thick.

The finger type cryostat also contains part of the input stage of the FET amplifier, the rest of the unit being in a box mounted on the cryostat, at the end opposite the detector. The vacuum inside the cryostat is maintained below 5.10^{-7} mm Hg by means of a molecular sieve and an ion pump.

Energy resolution of the detector is nominally 0.95 keV FWHM for the 122 keV gamma from Co-57, and 2.20 keV for the 1333 keV gamma from Co-60, although slightly better values than these have been attained quite often in normal running conditions.

With a detector of these dimensions, the photopeak to Compton ratios have been appreciably better than those obtained with the 0.5 cm^3 detector used previously. Fig. 4 shows spectra of the 2190 keV photopeak from Ce-144 and part of the Compton continuum for both detectors. Because of the better resolution of the new detector, the curves have been normalised so that the respective photopeaks have the same area.

Fig. 5 shows photopeak counting efficiency curves obtained for the two detectors, using calibrated IAEA gamma counting standards at a distance of 3 cm from the detector. The measurements on the 0.5 cm^3 detector were performed with a 2 mm thick lead sheet in front of the detector to harden the spectrum.

A plastic detector of diameter 27 cm, length 27 cm and provided with an axial hole 6 cm in diameter, is used as the anti-coincidence shield. Although this is fairly small with respect to stopping power for Compton-scattered gamma photons of higher energy, it was felt that larger sizes would be more inconvenient from the point of view of the extra weight of the detector and, particularly, the necessary shielding. Three 2" EMI 6097 photomultipliers are attached to the rear end of the detector. The semi-conductor in its cryostat hood (outer diameter 58 mm) can be easily slid into the axial hole of the plastic detector, with a play of 1 mm at each side. Shielding, consisting of three 4 cm thick steel plates and 5 cm lead bricks, covers only the sides, top and front of the detector assembly, which stands on a 5 cm thick steel table.

A block diagram of the complete counting system is shown in Fig. 6.

4. SCANNING RESULTS

Initially, it was thought that for scanning irradiated fuel rods, the plastic detector would have to be employed, using a mechanical device for sliding the whole assembly sideways to bring the semi-conductor detector back into the collimated gamma beam after completion of the scan. It was found, however, that excellent profiles could be obtained by using the output of the Ge(Li) detector itself. The dashed lines in Fig. 6 show how the units were connected. Before scanning, the gamma spectrum was obtained by means of the multi-channel analyser and the bias amplifier was then used to set the threshold energy to a suit-

able value. After this, the pulses from the bias amplifier were fed to the discriminator, whose threshold was set at 0 volts: from the discriminator constant amplitude pulses corresponding to all gamma photons over the original threshold energy, went to the ratemeter and then to the chart recorder. The chart speed of the recorder was selected to give a 1:1 scale factor, so that the length of the activity profile was the same as that of the fuel specimen. In order to avoid overloading the Ge(Li) detector and having too high a dead-time, lead sheets of varying thickness can be placed between the detector and the collimator.

Fuel rods of several different types have been scanned: Fig. 7 shows the activity profile obtained from a small fuel rod containing enriched UO_2 pellets which had Gd_2O_3 distributed homogenously in them. The bias amplifier settings had been selected so that all gamma photons over 380 keV were scanned. Very clearly resolved in the profile are the Zircaloy end-plugs (which are gamma active with Zr-95 due to the n,γ reaction on stable Zr-94) the positions of the three cobalt monitors, and the inter-pellet gaps, which permit identification of all 13 pellets in the rod. The extremely high end-effects are particularly interesting, since their heights were much larger than in the profile obtained with the conventional NaI detector scanner in the hot-cells, which uses a faster scanning speed.

Since the counting rates at the extreme ends of the fuel were different by more than a factor of two, it was necessary to confirm that the profiles was not distorted due to different deadtimes along the fuel. On several fuel rods, point measurements have been performed along the rods using the multichannel analyzer, which automatically allows for the dead-time. The normalised results showed excellent agreement with the activity profile scans.

In the case of fuel specimens where cobalt wire flux monitors are fitted in grooves around some of the pellets, the shape of the activity profile can be checked by measuring the Co-60 activity from the monitors. Fig. 8 shows a further profile on the rod shown in Fig. 7: in this case the energy threshold had been raised to 1000 keV, so that most of the pulses to the ratemeter were from the Co-60 gammas at 1173 keV and 1333 keV. It can be seen that the profile due to the fuel has been considerably reduced, representing only gamma photons from La-140 and Ce-144, and the approximate activities of the cobalt flux monitors can be readily measured.

5. ANTI-COINCIDENCE OPERATION

Once it had been shown that good profiles were obtainable, in which the position of the individual pellets could be located, the reduction of the Compton continuum by means of anti-coincidence operation was attempted.

The literature contains several descriptions of anti-coincidence systems for Ge(Li) detectors: Sever and Lippert (5) used a NaI well detector of 108 mm diameter as a guard detector, with both the semiconductor detector and radioactive source inside the crystal well, which was impracticable in our case. They obtained a Compton reduction of about 90 % at the Ccmpton edge, decreasing to about 30 % just below the back-scatter peak. Hill (6) used a very large plastic well detector, 660 mm diameter and 610 mm thick, to detect the Compton scattered photons, and obtained reductions in the Compton continuum better than 90 % at the Compton edge and about 85 % below the back-scatter peak. The whole assembly was housed in a massive steel and lead shield, and the Ge(Li) detector was lowered into the well by a pulley system. The radioactive source examined was internally located in the well of the plastic detector.

Figs. 9 and 10 show spectra without and with anti-coincidence respectively of an irradiated 2 % PuO_2. UO_2 fuel specimen obtained with our system. A reduction in the Compton continuum of about 50 % over the 500 - 1600 keV range was attained. Although not shown in the spectrum, a similar reduction applied down to about 300 keV. It can be seen that even after the relatively short cooling time of 4 months, the peaks from Ru-106 at 513, 624, 870, 1050, 1127 and 1565 keV are well resolved, and even the Cs-137 peak at 662 keV can be seen. Other peaks present are the 498 keV peak from Ru-103, the peaks at 724 and 758 keV from Zr-95, at 769 keV from Nb-95, at 1490 keV from Ce-144 and 1596 keV from La-140. The lower and less steeply sloping Compton continuum in Fig. 10 permits the determination of the activities of the peaks with greater precision than when the detector is operated as a straightforward photopeak spectrometer.

The larger decrease (about a factor of 4) in the height of the 1168 keV peak, which is the double escape peak from the 2190 keV gamma from Ce-144, should be noted. Since two 511 keV photons are emitted in pair production, the chance of <u>one</u> of them being detected in the plas-

tic shield detector, and hence cancelling the double escape peak pulse from the Ge(Li) detector, is correspondingly greater. Thus the possibility mentioned in the introduction of using the ratio of the 1050 keV and 1168 keV peaks as a measure of the relative fissions in U-235 and Pu-239 is only valid when the spectrometer is operated without anti-coincidence shielding.

However, the Ru-106 activity can be compared with other peaks, such as the 2190 keV peak from Ce-144, when operating in the anti-coincidence mode. The enhanced Ru-106 activity associated with Pu-239 fission can be seen by comparing Fig. 10 with Fig. 11, which is the spectrum from a UO_2 fuel rod, irradiated and cooled for the same time as the $PuO_2 . UO_2$ specimen. In order to facilitate comparison, the spectrum in Fig. 11 has been replotted so that the height of the 769 keV peak is approximately the same as in Fig. 10.

6. DISCUSSION

It is thought that the reduction in the Compton continuum with this counting arrangement is quite satisfactory. The plastic detector used is fairly small and therefore greater escape of the Compton scattered photons of higher energy is to be expected. Since these are associated with low energy Compton electrons in the Ge(Li) detector, improvement at the low energy end of the continuum will not be as large.

Attenuation of Compton scattered photons of low energy in the n-type and p-type layers of the detector, the mounting and the 2 mm thick aluminium of the cryostat hood reduces the reduction attainable at the Compton edge. However, the need for robustness and the use of an external collimated source, forces the compromise chosen.

Compared with the earlier detector of 0.5 cm^3 sensitive volume, the total reduction in the Compton continuum attained by using anti-coincidence shielding, together with the reduction achieved by using a larger detector, is about 75 % and this substantially improves the measurement precision.

The modified transport flask has been shown to function well as a gamma scanner, and the facility presents the opportunity of examining small irradiated fuel specimens without the complications of background level often associated with work near hot-cell facilities, and without disturbing work routines. Some type of similar system could be of in-

terest in the application of Safeguards, the control of fissile material, to irradiated fuel elements. By reference to the activity profile, individual fuel pellets can be located and examined.

Consideration is currently being given to manufacturing a more permanent steel shield for the detector assembly which will fit mechanically on to the collimator of the transport flask. This would ensure a constant geometry with respect to the fuel specimen so that, after suitable calibration, quantitative, non-destructive determination of fission product activities in the fuel, and hence the burn-up, could be effected.

REFERENCES

1. FORSYTH R S, BLACKADDER W H and RONQVIST N,
Burn-up determination by high resolution gamma spectrometry: Axial and diametral scanning experiments. 1967.
(AE-267).

2. FORSYTH R S, BLACKADDER W H and RONQVIST N,
Burn-up determination by high resolution gamma spectrometry: Fission product migration studies. 1967.
(AE-272).

3. FORSYTH R S and BLACKADDER W H,
Use of the fission product Ru-106 gamma activity as a method for estimating the relative number of fission events in U-235 and Pu-239 in low-enriched fuel elements. 1970.
(AE-390).

4. KATCOFF S,
Fission-product yields from neutron-induced fission.
Nucleonics 18 (1960):11, p. 201.

5. SEVER Y and LIPPERT J,
A compton-rejection germanium spectrometer.
Nucl. Instr. Methods 33 (1965) p. 347.

6. HILL M W,
An anticoincidence-shielded Ge(Li) gamma-ray spectrometer.
Nucl. Instr. Methods 36 (1965) p. 350.

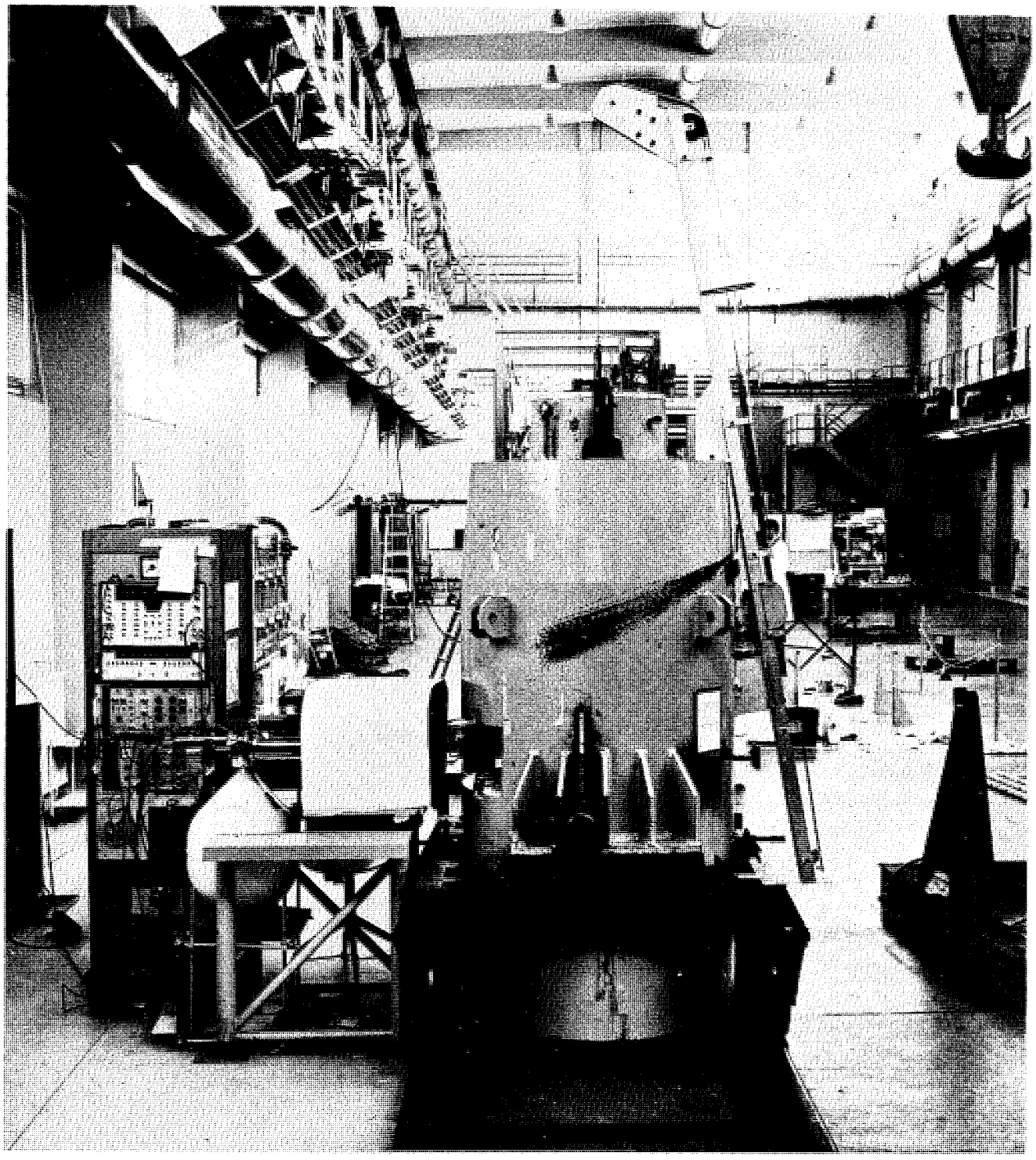

Fig. 1

General view of the transport flask and spectrometer

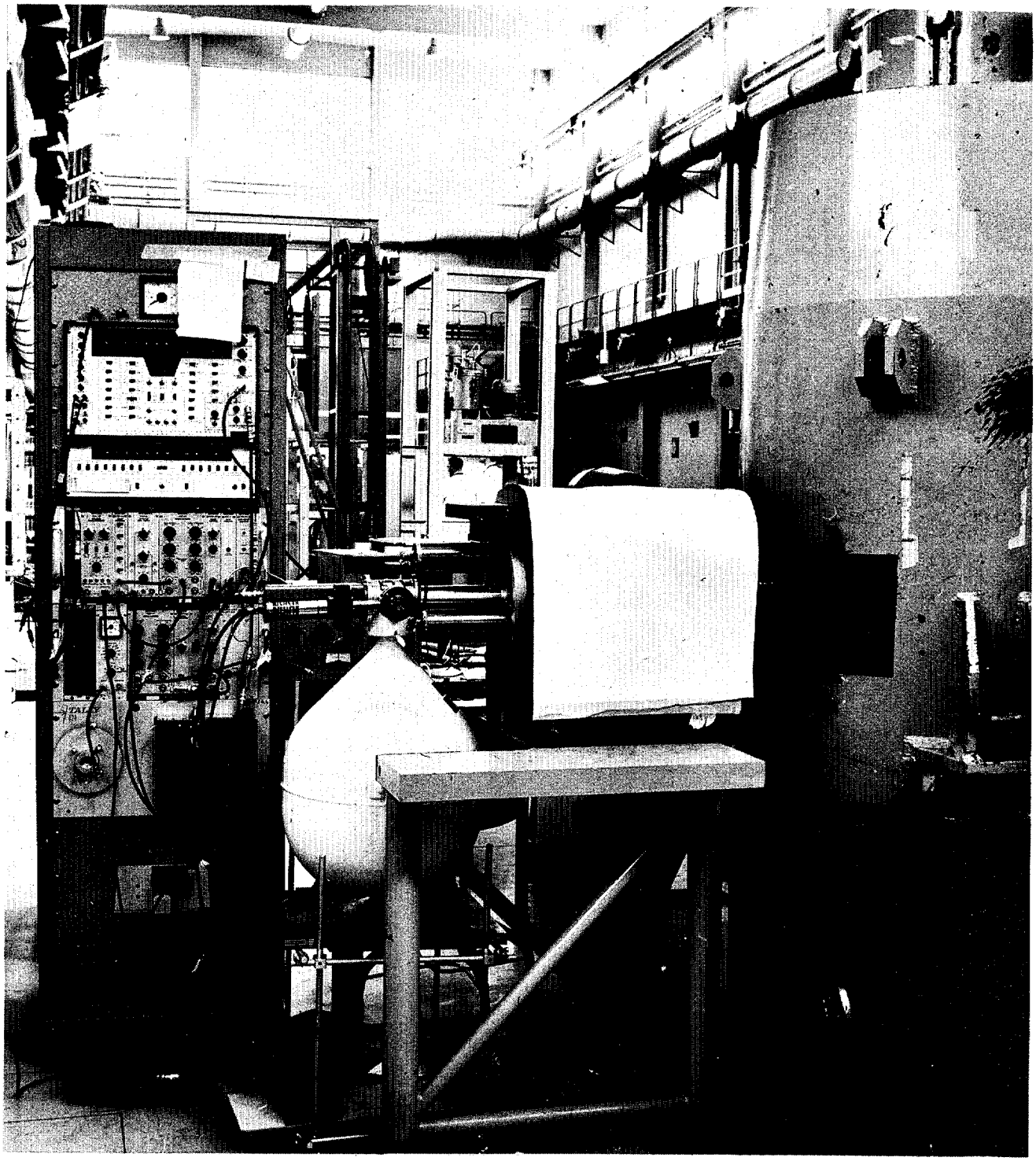

Fig. 2

View of the spectrometer showing anti-coincidence crystal in position

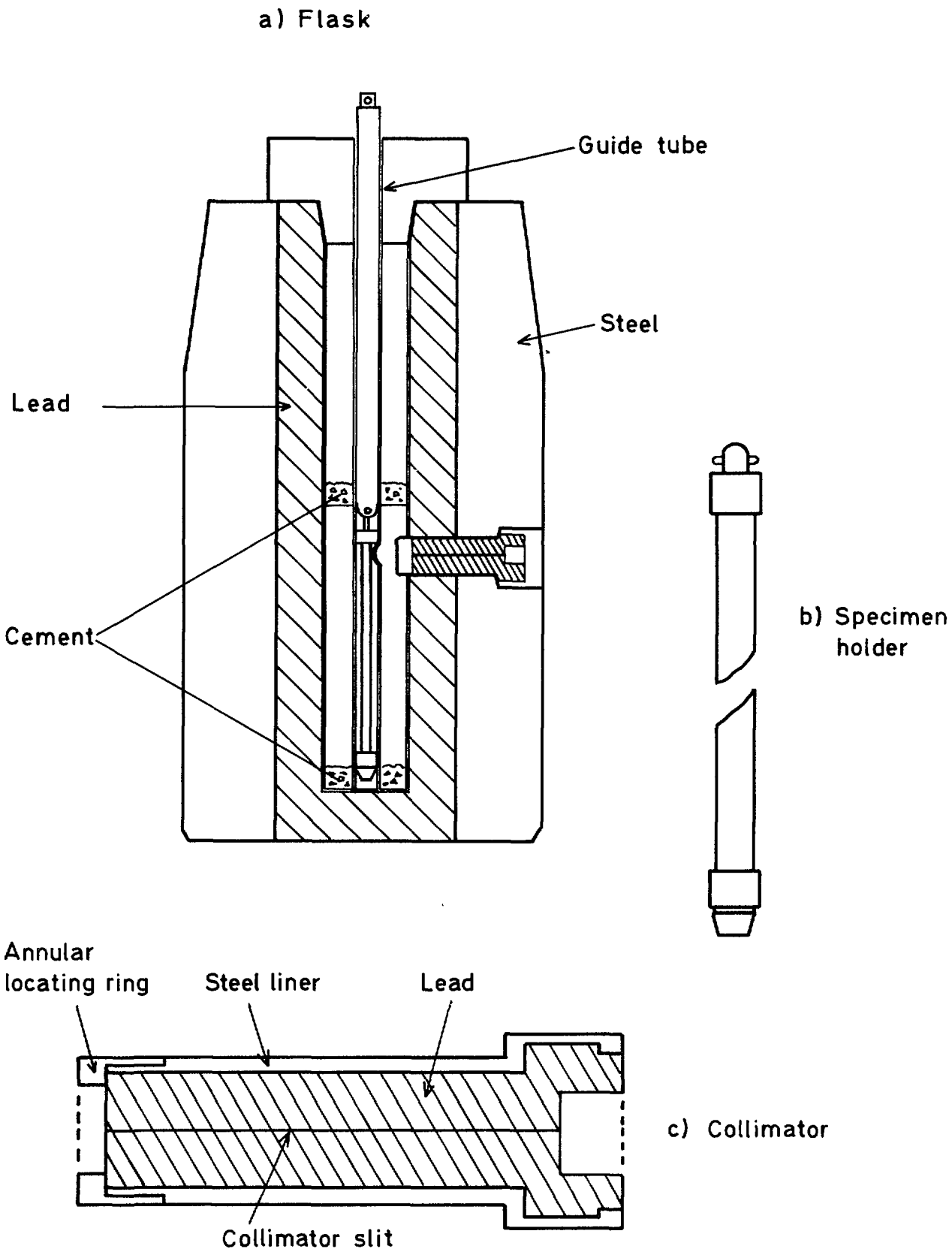

Fig. 3 Sketch of scanning assembly.

Fig. 4 Comparison of Compton continuum levels for old and new detectors. (Equal counts in 2190 keV photopeak)

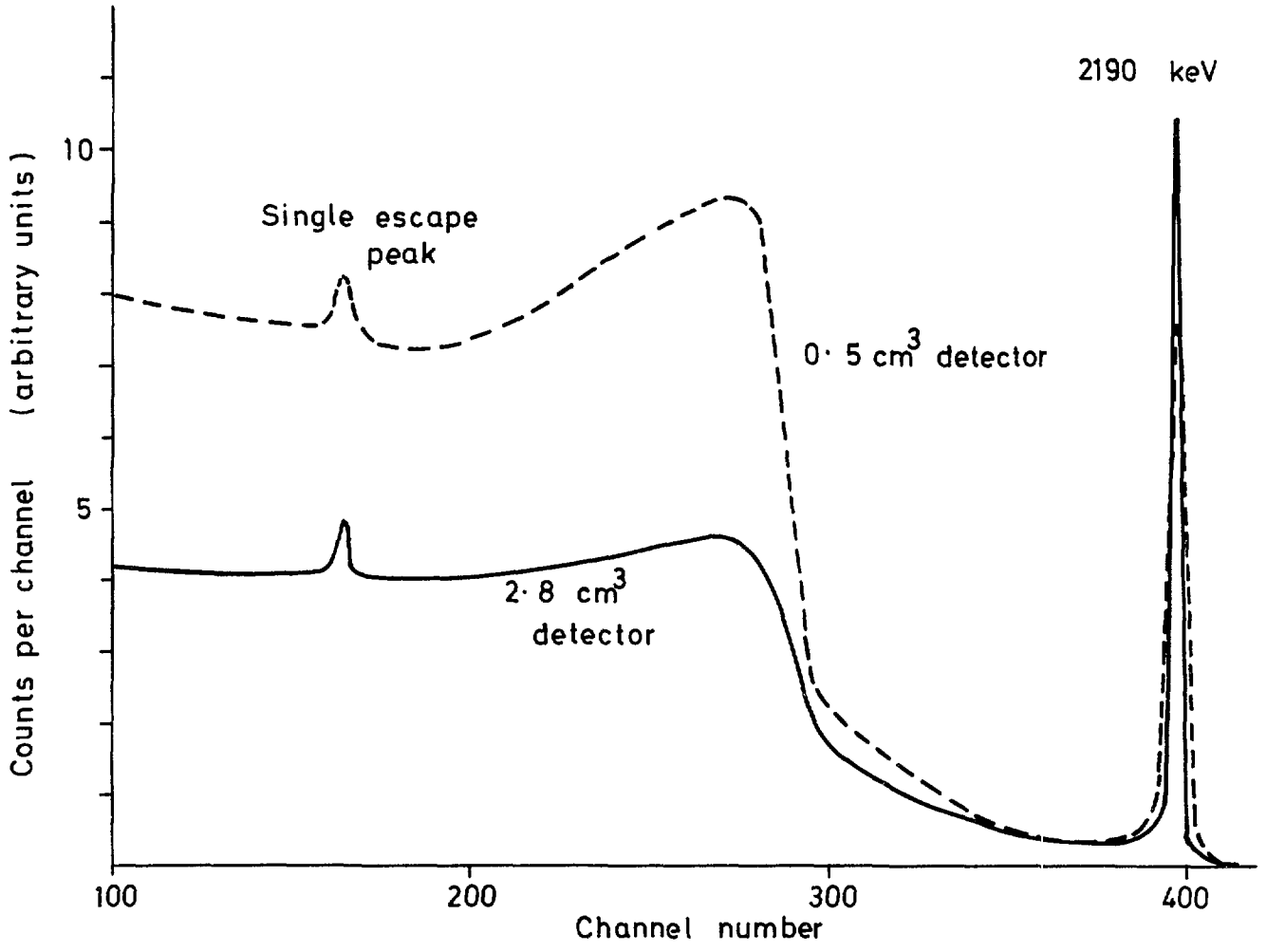

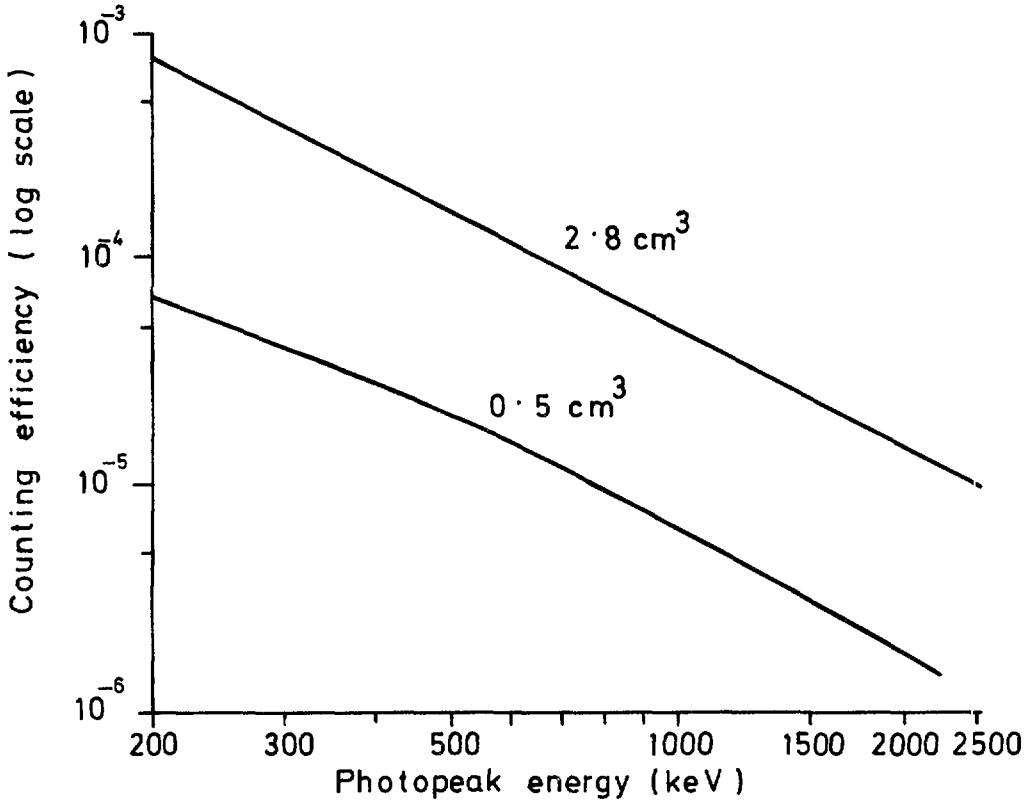

Fig. 5 Comparison of photopeak counting efficiencies for old and new detectors

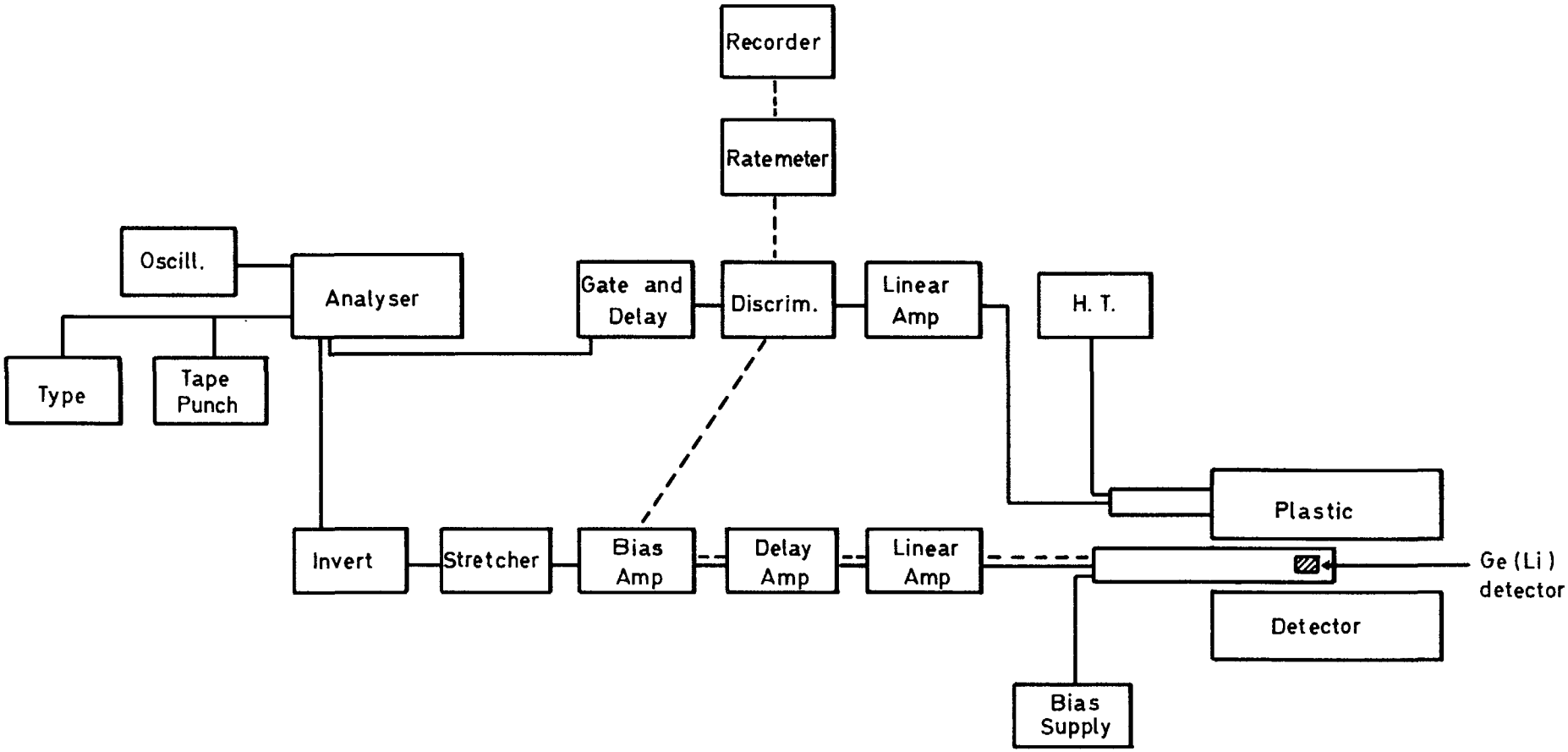

Fig. 6 Block diagram of the anti-coincidence system.
Dashed lines show coupling for profile scanning.

Fig. 7

Gamma activity profile of an irradiated fuel rod containing UO_2 pellets poisoned with Gd_2O_3. Discriminator setting: 380 keV

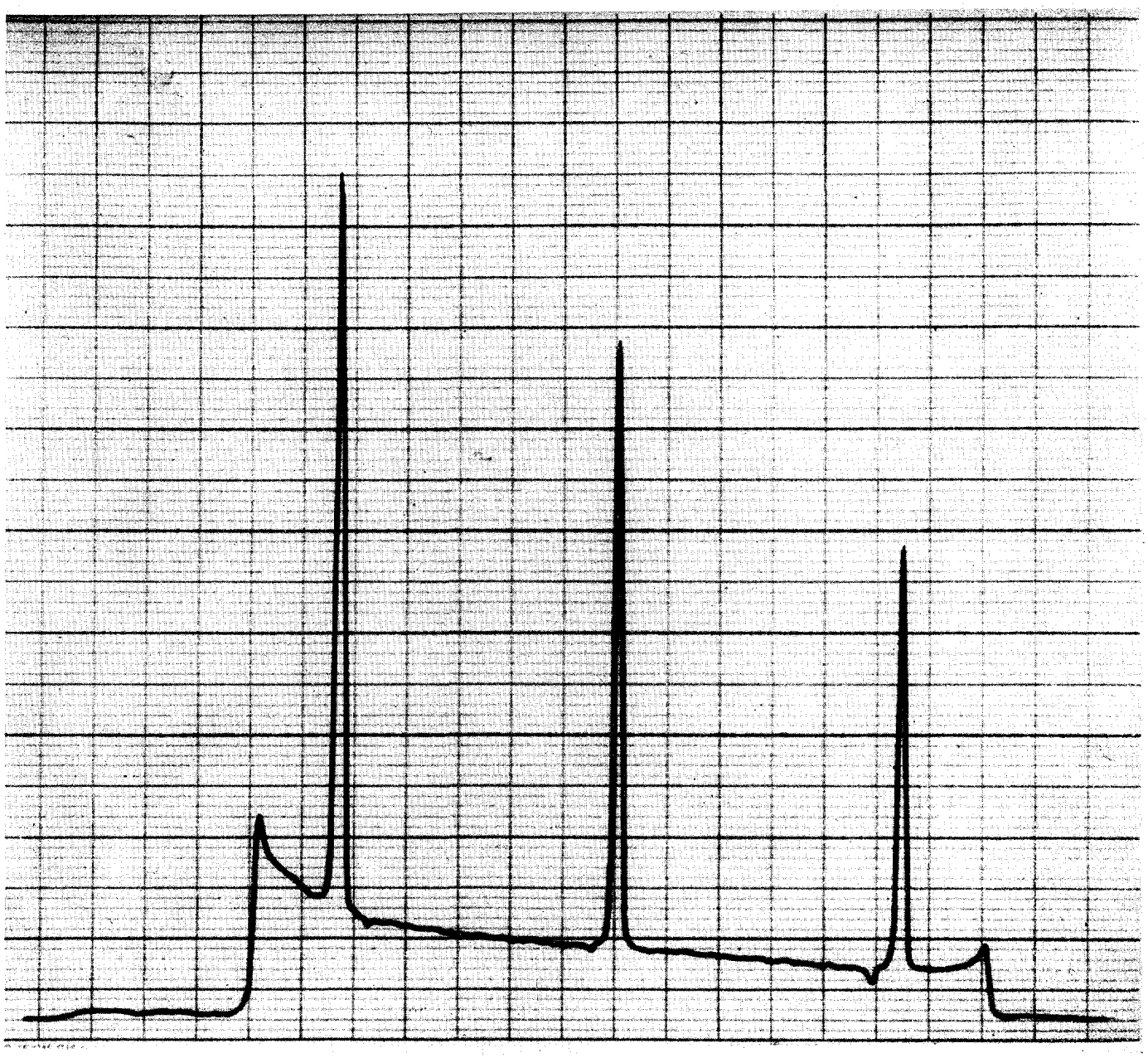

Fig. 8

Gamma activity profile of rod shown in Fig. 7, but with discriminator setting: 1000 keV. Cobalt monitor activities are clearly shown

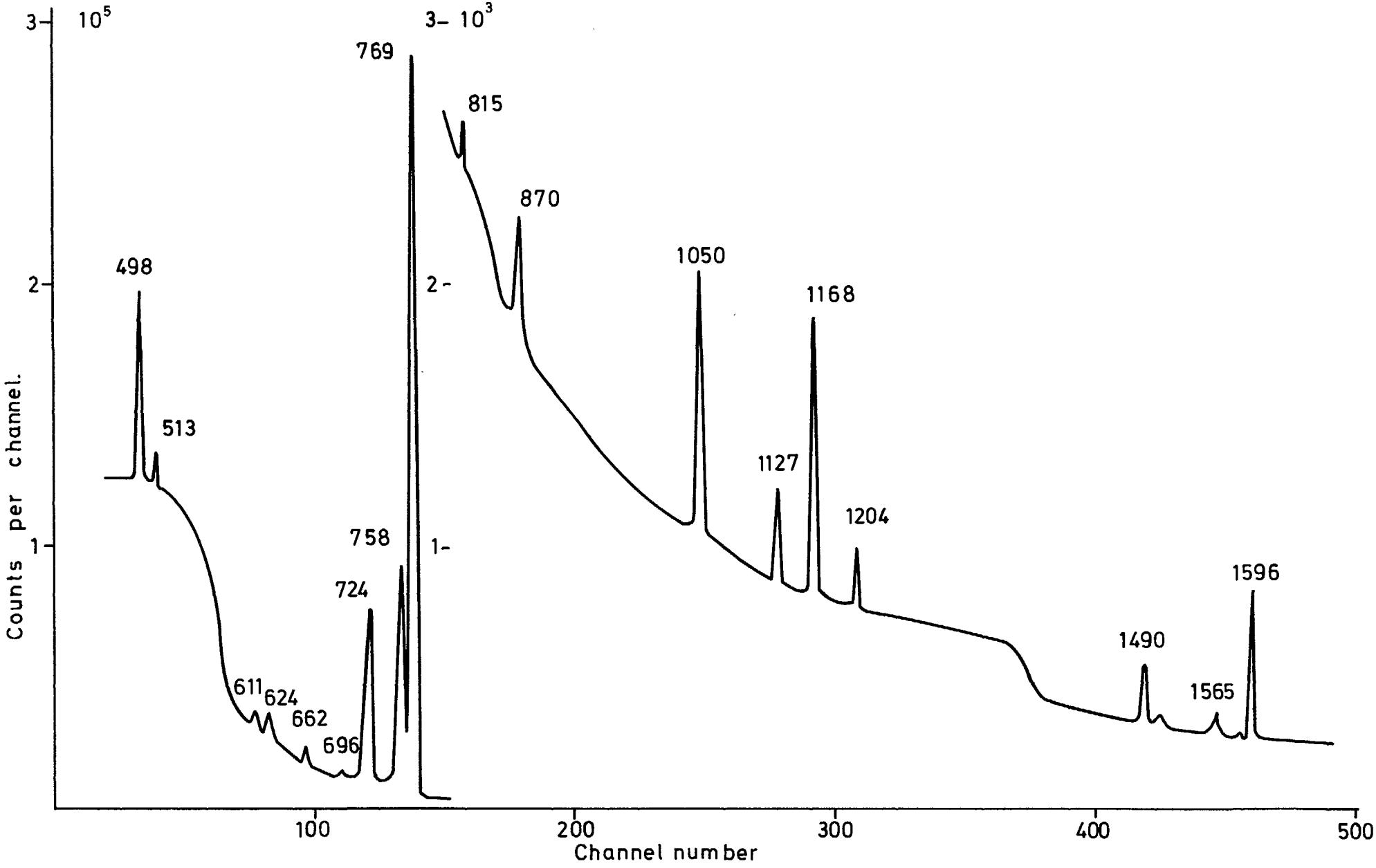

Fig. 9 Spectrum from 2 % $PuO_2.UO_2$ fuel rod. Without anti - coincidence.

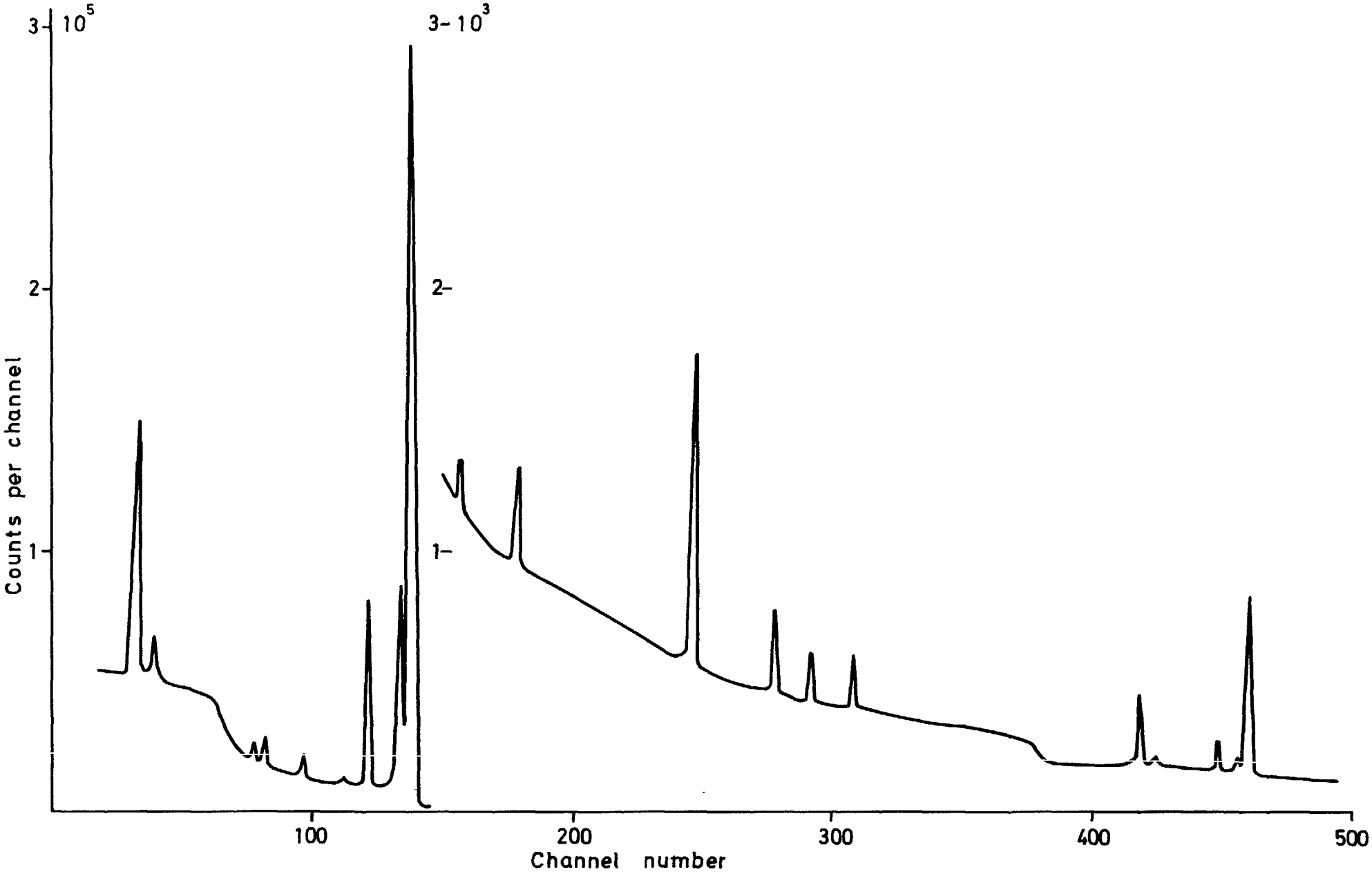

Fig. 10 Spectrum from 2% $PuO_2 . UO_2$ fuel rod. With anti-coincidence.

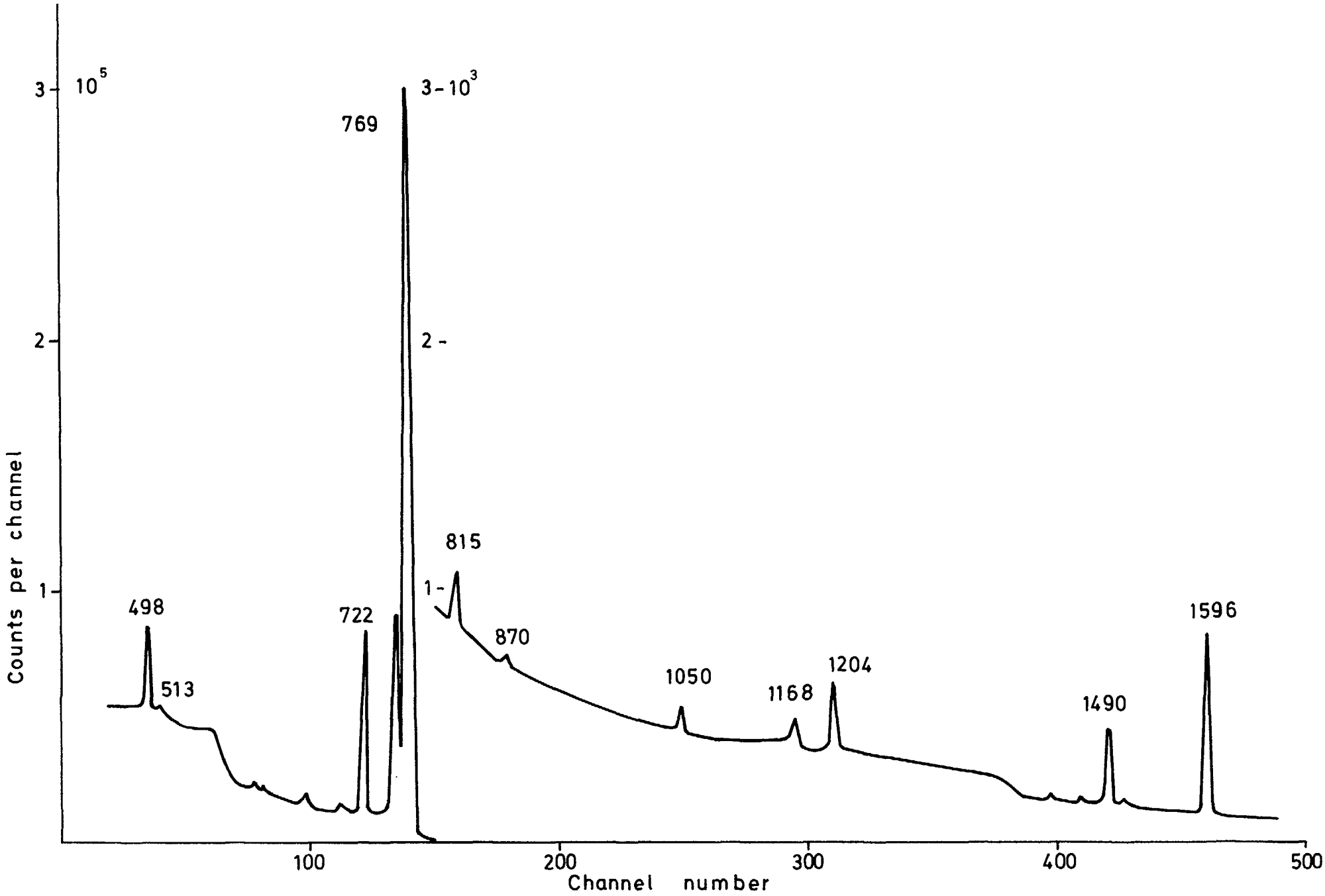

Fig 11. Spectrum from UO_2 fuel rod (3 % U - 235). With anti - coincidence.

LIST OF PUBLISHED AE-REPORTS

1–320 (See back cover earlier reports.)

321 Stability of a steam cooled fast power reactor, its transients due to moderate perturbations and accidents. By H. Vollmer. 1968. 36 p. Sw. cr. 10:–.

322. Progress report 1967. Nuclear chemistry. 1968. 30 p. Sw. cr. 10:–.

323 Noise in the measurement of light with photomultipliers. By F. Robben. 1968. 74 p. Sw. cr. 10:–.

324. Theoretical investigation of an electrogasdynamic generator. By S. Palmgren. 1968 36 p. Sw. cr. 10:–.

325. Some comparisons of measured and predicted primary radiation levels in the Agesta power plant. By E. Aalto, R Sandlin and A. Krell. 1968. 44 p. Sw. cr. 10:–.

326. An investigation of an irradiated fuel pin by measurement of the production of fast neutrons in a thermal column and by pile oscillation technique. By Veine Gustavsson. 1968 24 p. Sw. cr. 10:–.

327. Phytoplankton from Tvären, a bay of the Baltic, 1961–1963. By Torbjörn Willén. 1968. 76 p. Sw. 10:–.

328. Electronic contributions to the phonon damping in metals. By Rune Jonson. 1968. 38 p. Sw cr. 10:–.

329. Calculation of resonance interaction effects using a rational approximation to the symmetric resonance line shape function. By H. Häggblom. 1968. 48 p. Sw. cr 10:–.

330. Studies of the effect of heavy water in the fast reactor FR0. By L. I. Tirén, R. Håkansson and B. Karmhag. 1968. 26 p. Sw. cr. 10:–.

331. A comparison of theoretical and experimental values of the activation Doppler effect in some fast reactor spectra. By H. Häggblom and L. I. Tirén. 1968. 28 p. Sw. cr. 10:–.

332. Aspects of low temperature irradiation in neutron activation analysis. By D Brune. 1968. 12 p. Sw. cr. 10.–.

333. Application of a betatron in photonuclear activation analysis. By D. Brune, S. Mattsson and K. Lidén. 1968. 13 p. Sw. cr. 10:–.

334 Computation of resonance-screened cross section by the Dorix-Speng system. By H Häggblom. 1968. 34 p. Sw. cr. 10:–.

335. Solution of large systems of linear equations in the presence of errors. A constructive criticism of the least squares method. By K. Nygaard. 1968. 28 p. Sw. cr 10:–.

336 Calculation of void volume fraction in the subcooled and quality boiling regions. By S. Z. Rouhani and E. Axelsson. 1968. 26 p. Sw. cr. 10:–.

337. Neutron elastic scattering cross sections of iron and zinc in the energy region 2.5 to 8.1 MeV. By B. Holmqvist, S. G. Johansson, A. Kiss, G. Lodin and T. Wiedling. 1968. 30 p. Sw. cr. 10:–.

338. Calibration experiments with a DISA hot-wire anemometer. By B. Kjellström and S. Hedberg. 1968. 112 p. Sw. cr. 10:–.

339 Silicon diode dosimeter for fast neutrons. By L. Svansson, P. Swedberg, C-O. Widell and M. Wik. 1968. 42 p. Sw. cr. 10:–.

340 Phase diagrams of some sodium and potassium salts in light and heavy water. By K. E. Holmberg. 1968 48 p. Sw. cr. 10:–.

341. Nonlinear dynamic model of power plants with single-phase coolant reactors. By H. Vollmer. 1968. 26 p. Sw. cr. 10:–.

342. Report on the personnel dosimetry at AB Atomenergi during 1967. By J. Carlsson and T. Wahlberg. 1968. 10 p. Sw. cr. 10:–.

343. Friction factors in rough rod bundles estimated from experiments in partially rough annuli – effects of dissimilarities in the shear stress and turbulence distributions. By B. Kjellström. 1968. 22 p. Sw. cr. 10:–.

344. A study of the resonance interaction effect between ^{238}U and ^{239}Pu in the lower energy region. By H. Häggblom. 1968. 48 p. Sw. cr. 10:–.

345. Application of the microwave discharge modification of the Wilzbach technique for the tritium labelling of some organics of biological interest By T. Gosztonyi. 1968. 12 p. Sw. cr. 10:–.

346 A comparison between effective cross section calculations using the intermediate resonance approximation and more exact methods. By H. Häggblom. 1969. 64 p. Sw. cr. 10:–.

347. A parameter study of large fast reactor nuclear explosion accidents. By J. R Wiesel. 1969. 34 p. Sw. cr. 10:–.

348. Computer program for inelastic neutron scattering by an anharmonic crystal By L. Bohlin, I. Ebbsjö and T. Högberg. 1969. 52 p. Sw. cr. 10:–.

349. On low energy levels in ^{185}W. By S G. Malmskog, M. Höjeberg and V Berg. 1969. 18 p. Sw. cr. 10:–.

350. Formation of negative metal ions in a field-free plasma. By E. Larsson 1969. 32 p. Sw. cr 10:–.

351. A determination of the 2 200 m/s absorption cross section and resonance integral of arsenic by pile oscillator technique. By E. K. Sokolowski and R Bladh. 1969. 14 p Sw. cr. 10:–.

352. The decay of ^{191}Os. By S. G Malmskog and A. Bäcklin. 1969. 24 p. Sw cr 10:–.

353 Diffusion from a ground level point source experiment with thermoluminescence dosimeters and Kr 85 as tracer substance. By Ch. Gyllander, S Hollman and U. Widemo 1969. 23 p. Sw. cr. 10:–

354 Progress report, FFN, october 1, 1967 – september 30, 1968 By T. Wiedling. 1969. 35 p. Sw. cr. 10:–.

355. Thermodynamic analysis of a supercritical mercury power cycle. By A. S Roberts, Jr., 1969. 25 p. Sw. cr. 10:–.

356. On the theory of compensation in lithium drifted semiconductor detectors By A. Lauber. 1969. 45 p. Sw cr 10:–

357 Half-life measurements of levels in ^{75}As. By M. Höjeberg and S. G. Malmskog. 1969. 14 p Sw. cr 10:–.

358. A non-linear digital computer model requiring short computation time for studies concerning the hydrodynamics of the BWR. By F. Reisch and G Vayssier. 1969. 38 p. Sw. cr. 10: –

359. Vanadium beta emission detectors for reactor in-core neutron monitoring. I. Ö. Andersson and B. Söderlund. 1969. 26 p. Sw. cr. 10:–.

360. Progress report 1968 nuclear chemistry. 1969. 38 p. Sw. cr. 10:–.

361. A half-life measurement of the 343.4 keV level in ^{175}Lu. By M. Höjeberg and S. G Malmskog. 1969. 10 p. Sw. cr. 10:–.

362. The application of thermoluminescence dosimeters to studies of released activity distributions. By B-I. Rudén. 1969. 36 p. Sw. cr. 10:–.

363. Transition rates in ^{161}Dy. By V Berg and S. G. Malmskog. 1969. 32 p. Sw. cr 10:–.

364. Control rod reactivity measurements in the Ågesta reactor with the pulsed neutron method. By K. Björeus. 1969. 44 p. Sw. cr. 10:–.

365. On phonons in simple metals II. Calculated dispersion curves in aluminium. By R. Johnson and A. Westin. 1969. 124 p. Sw. cr. 10:–.

366. Neutron elastic scattering cross sections. Experimental data and optical model cross section calculations A compilation of neutron data from the Studsvik neutron physics laboratory. By B. Holmqvist and T. Wiedling. 1969. 212 p. Sw. cr 10:–.

367 Gamma radiation from fission fragments. Experimental apparatus – mass spectrum resolution. By J. Higbie. 1969. 50 p. Sw. cr. 10:–.

368. Scandinavian radiation chemistry meeting Studsvik and Stockholm, september 17–19, 1969. By H. Christensen. 1969. 34 p. Sw cr. 10:–.

369. Report on the personnel dosimetry at AB Atomenergi during 1968. By J. Carlsson and T Wahlberg. 1969. 10 p. Sw. cr 10:–.

370. Absolute transition rates in ^{188}Ir. By S G. Malmskog and V. Berg. 1969. 16 p Sw. cr. 10:–.

371. Transition probabilities in the 1/2+(631) Band in ^{235}U. By M. Höjeberg and S. G. Malmskog. 1969. 18 p. Sw. cr. 10:–.

372. E2 and M1 transition probabilities in odd mass Hg nuclei. By V. Berg, A. Bäcklin, B. Fogelberg and S. G Malmskog. 1969. 19 p. Sw. cr. 10:–.

373. An experimental study of the accuracy of compensation in lithium drifted germanium detectors. By A. Lauber and B. Malmsten. 1969. 25 p. Sw. cr. 10:–.

374. Gamma radiation from fission fragments. By J. Higbie. 1969. 22 p Sw. cr. 10:–.

375 Fast Neutron Elastic and Inelastic Scattering of Vanadium. By B. Holmqvist, S. G. Johansson, G. Lodin and T. Wiedling. 1969. 48 p. Sw. cr. 10:–.

376. Experimental and Theoretical Dynamic Study of the Ågesta Nuclear Power Station. By P.-Å. Bliselius, H. Vollmer and F. Åkerhielm. 1969. 39 p. Sw. cr. 10: –

377. Studies of Redox Equilibria at Elevated Temperatures 1. The Estimation of Equilibrium Constants and Standard Potentials for Aqueous Systems up to 374°C. By Derek Lewis. Sw. cr. 10:-

378. The Whole Body Monitor HUGO II at Studsvik. Design and Operation. By L. Devell, I. Nilsson and L. Venner. 1970. 26 p. Sw. cr. 10:-.

379. ATOMSPHERIC DIFFUSION Investigations at Studsvik and Ågesta 1960–1963. By L-E Hæggblom, Ch Gyllander and U Widemo. 1969. 91 p. Sw. cr. 10: –

380. An expansion method to unfold proton recoil spectra. By J. Kockum. 1970. 20 p. Sw. cr. 10: –.

381. The 93. 54 keV level in ^{91}Sr, and evidence for 3-neutron states above N=50. By S. G. Malmskog and J. Mc Donald. 1970. 24 p. Sw. cr. 10:-.

382. The low energy level structure of ^{191}Ir. By S. G. Malmskog, V. Berg, A. Bäcklin and G. Hedin. 1970. 24 p. Sw. cr. 10:–.

383. The drinking rate of fish in the Skagerack and the Baltic. J. E. Larsson. 16 p. Sw. cr. 10: –.

384. Lattice dynamics of NaCl, KCl, RbCl and RbF. G. Raunio and S. Rolandson 26 p. Sw. cr. 10: –.

385. A neutron elastic scattering study of chromium, iron and nickel in the energy region 1.77 to 2.76 MeV. 26 p. By B. Holmqvist, S .G Johansson, G. Lodin, M. Salama and T. Wiedling. 1970. Sw. cr. 10: –

386. The decay of bound isobaric analogue states in ^{28}Si and ^{32}S using (d, nγ) reactions. By L. Nilsson, A. Nilsson and I. Bergqvist. 1970. 34 p. Sw. cr. 10:–.

387. Transition probabilities in ^{189}Os. By S. G. Malmskog, V. Berg and A. Bäcklin. 1970. 40 p. Sw. cr. 10: –.

388. Cross sections for high-energy gamma transitions from MeV neutron capture in ^{206}Pb. By I. Bergqvist, B. Lundberg and L. Nilsson. 1970. 16 p. Sw. cr. 10: –.

389. High-speed, automatic radiochemical separations for activation analysis in the biological and medical research laboratory. By K. Samsahl. 1970. 18 p. Sw. cr. 10: –.

390. Use of fission product Ru-106 gamma activity as a method for estimating the relative number of fission events in U-235 and Pu-239 in low-enriched fuel elements. By R. S. Forsyth and W. H. Blackadder. 1970. 26 p. Sw. cr. 10: –.

391. Half-life measurements in ^{134}I. By V. Berg and Å. Höglund. 1970. 16 p. Sw. cr. 10: –.

392. Measurement of the neutron spectra in FR0 cores 5, 9 and PuB-5 using resonance sandwich detectors. By T. L. Andersson and M. N. Qazi. 1970. 30 p. Sw. cr. 10: –.

393. A gamma scanner using a Ge(Li) semi-conductor detector with the possibility of operation in anti-coincidence mode. By R. S. Forsyth and W. H. Blackadder. 1970. 22 p. Sw. cr. 10: –.

List of published AES-reports (In Swedish)

1. Analysis be means of gamma spectrometry. By D. Brune. 1961. 10 p. Sw. cr. 6:–.
2. Irradiation changes and neutron atmosphere in reactor pressure vessels-some points of view. By M. Grounes. 1962. 33 p. Sw cr. 6:–.
3. Study of the elongation limit in mild steel. By G. Östberg and R. Attermo. 1963 17 p. Sw. cr. 6:–.
4. Technical purchasing in the reactor field. By Erik Jonson. 1963. 64 p. Sw. cr. 8:–.
5. Ågesta nuclear power station. Summary of technical data, descriptions, etc. for the reactor. By B. Lilliehöök. 1964. 336 p. Sw. cr. 15:–.
6. Atom Day 1965. Summary of lectures and discussions. By S. Sandström. 1966. 321 p. Sw. cr. 15:–.
7. Building materials containing radium considered from the radiation protection point of view. By Stig O W. Bergström and Tor Wahlberg. 1967. 26 p. Sw. cr. 10:–.

Additional copies available from the library of AB Atomenergi, Fack, S-611 01 Nyköping, Sweden.

EOS-tryckerierna, Stockholm 1970